eISSN: 2976-1190

Journal of Engineering and Sciences

Vol. 3 Issue 1 May 30, 2024 / **DOI: https://doi.org/10.3126/jes2.v3i1.66233**

Journal homepage: Journal of Engineering and Sciences (nepjol.info)

Publisher: Research Management Cell, Pashchimanchal Campus, Lamachour, Pokhara

Urban Roadside Flooding Analysis Using SWMM: A Case Study of a Road Section in Pokhara Metropolitan City, Nepal

Aavas Jung Shahi[1], Madan Pokhrel[2,*], Shankar Lamichhane[1]

[1]*School of Engineering, Faculty of Science and Technology Pokhara University, Nepal*

[2]*Paschimanchal Campus, Institute of Engineering, Tribhuvan University*

(Manuscript Received 17/03/2024; Revised 19/05/2024; Accepted 26/05/2024)

Abstract

Pokhara City, in Nepal, experiences heavy rainfall during four months of monsoon, causing stress on drainage infrastructures. This situation is exacerbated by poor drainage systems, ineffective urban planning, and rapid urbanization. This study aims to develop mitigation strategies for urban roadside flooding in the Barahi Chowk region in Pokhara City. The focus is to identify the causes and potential solutions for the recurring issue of urban roadside flooding. For this purpose, the study utilizes Storm Water Management Model (SWMM) computer modeling to analyze the hydraulic capacity of existing drainage systems during peak flows. The SWMM modeling reveals that the current drainage usage is between 80% and 100% during peak times, leading to flooding. Consequently, resizing or expanding various drainage sections using SWMM modeling is suggested. The study introduces Low Impact Development (LID) controls, such as rain gardens and permeable pavements, to manage surface runoff. Implementing rain gardens on just 3% of the impervious area in each sub-catchment showed an average 21.5% reduction in peak runoff and an average 6.68% reduction in the total runoff while implementing 5% in each sub-catchment, permeable pavements reduced peak runoff by 22-26% and total runoff by 8-11%. The research explores the impact of land use and land cover change and unplanned urban growth on roadside flooding, resulting in impermeable urban surfaces that disturb the natural drainage system and infiltration pattern. Thus, the outcomes of this study should be carefully considered by policymakers and stakeholders to address issues through sustainable urban planning and infrastructure development. Also, implementing measures like resizing drains and LID controls appears to be effective in controlling flooding during the study period and should be considered for future studies as well.

Keywords: Urban flooding; SWMM; LID; Roadside flooding; Pokhara city

1. Introduction

Nepal has a climate with a strong summer monsoon and a relatively dry winter. It receives about 80% of its annual rainfall during the four months of the monsoon [1]. Historically, due to reliance on agriculture, several of its cities once had sizable agricultural areas. Because the agricultural land naturally allowed rainwater to seep into the ground, it acted as a sponge that could absorb and hold onto water during periods of severe rainfall, which helped to reduce floods in the major urban regions [2]. However, in recent decades, the country has been experiencing rapid urbanization. Without any planning and urban policies, urban growth is characterized by haphazard expansion [3]. This has led to the disorganized construction of infrastructure such as roadways, industries, and residential areas, thus increasing the impermeable concrete and asphalt surface at the expense of permeable land. This has resulted in a quick runoff with a high peak and reduced the time of concentration for rainfall events leading to floods [4]. The situation is further exacerbated by climate change and the increase in extreme precipitation events [5], resulting in more frequent and severe roadside flooding and stress on the existing infrastructures.

Effective stormwater management can be a great asset to manage urban flooding and safeguard from the consequences of excessive rainfall. This is now critical to mitigate the impacts of urbanization and impervious surfaces. Various techniques have been utilized for this purpose, including efficient collection and stormwater runoff from households, and implementation of a separate stormwater disposal system leading to either stormwater drains or natural watercourses. Additionally, green infrastructure and stormwater management strategies can be great implementation measures to increase permeability and reduce impervious surfaces, thereby restoring natural water infiltration and minimizing the burden on

*Corresponding author. Tel.: +977- 9843624588,
E-mail address: madan@ioepas.edu.np

Figure 1: Roadside flooding during 2022 monsoon in the Barahi Chowk region

existing drainage systems [6-8]. Moreover, investing in resilient and well-designed stormwater management infrastructure can aid in mitigating the impacts of urbanization on flooding and ensure the sustainable development of cities in Nepal.

Modern stormwater management and urban drainage design heavily rely on advanced computer modeling software. These tools, including SWMM (Storm Water Management Model) [9], MOUSE [10], Info Works, HEC-RAS (Hydrologic Engineering Center's River Analysis System) [11], and HYKAS, offer integrated platforms for modeling, simulating, and designing drainage networks. These tools equip engineers and planners with powerful tools to analyze and comprehend the behavior of stormwater in urban areas, facilitating the development of efficient and effective drainage systems.

This study utilized the SWMM modeling technique to analyze the effectiveness of low-impact development strategies in one of the wettest regions in Nepal, Pokhara City. In their 2019 research, Khadka et al., 2018 investigated the issue of urban flooding in the lakeside area of Pokhara City, pinpointing the necessity to address runoff management for effective problem mitigation [12]. Similarly, Paudel and Dawadi, 2022 found that LID techniques, such as permeable concrete, were effective in reducing urban flooding in different parts of Pokhara City [13]. Consequently, this study delves into various techniques aimed at addressing this challenge. Specifically, the study focused on the Barahi Chowk area in the lakeside area, which includes numerous hotels and infrastructure to accommodate the large number of tourists visiting Pokhara City. The runoff produced during the heaviest rainfall was determined to be too much for the current drainage system in Barahi Chowk Lakeside. Therefore, this area holds socio-economic significance for both the city and the country.

The findings of this study could lead to strategic planning for mitigating the problem, thus reducing disruptions to traffic and economic activities in the region. Accurate modeling of urban drainage systems, as demonstrated in this study, is essential for urban planners, the metropolitan area, and other relevant bodies involved in the planning and administration of infrastructure.

2. Study Area

Pokhara, one of the biggest cities in Nepal, is a popular tourist destination with stunning natural surroundings. An enormous number of visitors, both domestic and foreign, arrive each year. Due to this, the number of individuals who visit, work, and transact business within the city grows significantly each year. Because of the city's scenic surroundings and socioeconomic significance to a large number of Nepalese, it holds many values. Based on available statistics, the average annual temperature in Pokhara is 18.3 °C, and the

location receives an average of 3300 mm of annual rainfall.

The Baharai Chowk study area lies in the northwest

Figure 3 Study Area (Barahi Chowk)

corner of Pokhara City, extending from 28º 12' 20" lat itude 83º 57' 39" longitude to 28º 12' 75" latitude 83º 57' 95" longitude. The catchment includes the northern part of the ward office to Nareshwor Chowk, extending up to Durbar Chowk, Mira Galli, and Barahai Chowk of Pokhara Metropolitan City. Due to unmanaged migration to the city from surrounding regions, it is experiencing rapid unplanned urbanization. The city is witnessing astronomical growth in impervious surfaces due to various construction activities, including the road network, buildings, and other infrastructures.

3. Materials and Method

Firstly, the study area was demarcated in Google Earth Pro. The total study area was measured using the measuring tools available in Google Earth Pro. The catchment was divided into different sub-catchment zones based on the slope, elevation, and drainage flow pattern. The area of each sub-catchment was also measured. The major existing drainage and street networks were marked within the catchment area in Google Earth Pro, which potentially receives the runoff from the sub-catchments. The size and shape of cross-sections of the existing drainage networks were measured in the field. The drainage system in the study area consisted of tick drains. The average size of a tick drain is 0.2m width × 0.1m curb height with a cross slope of 2-4%, which was used according to the site and condition of the drain. The implementation of drainage in the model is shown in Figure 3.

3.1 Frequency Analysis

The Gumbel method was adopted for the rainfall frequency analysis [14]. Maximum 24-hour duration

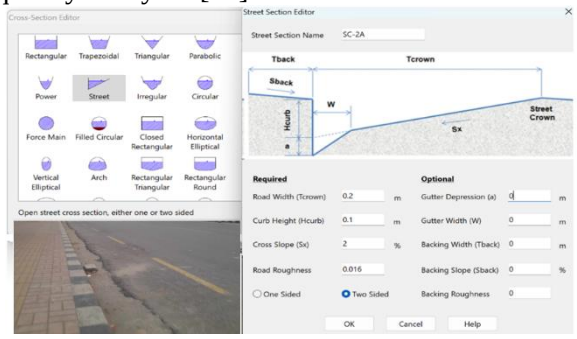

Figure 2: Existing tick-drain and its representation in the study area

Rainfall data from 2000 to 2023 of Airport Station (0804) of the Department of Hydrology and Meteorology was adopted for this purpose. The equation used for the frequency analysis is shown in Eq 1.

$$X_t = X_{mean} + \sigma K_t \quad \text{..... Eq 1}$$

where,

K_t = Frequency factor for T return period as given below

X_{mean} and X_t are the mean value of variate and value of variate at the return period of t.

$$K_t = \frac{(Y_t - \overline{Y_n})}{S_n} \quad \text{..... Eq 2}$$

$$Y_t = -\left[\ln \ln \frac{T}{T-1}\right] \quad \text{..... Eq 3}$$

$\overline{Y_n}$ and S_n reduced mean and reduced standard deviation in Gumbel's Extreme Value Distribution for n. These values are obtained from Gumbel's table for the given sample size. The Y_t is reduced variate.

Once the different return period flood was computed, the disintegration of this maximum twenty-four-hour rainfall is analyzed for various time intervals throughout the year. This analysis is conducted using an empirical formula suggested by the Indian Meteorological Department (IMD) [15].

$$P_t = P_{24} \times (t/24)^{1/3} \quad \text{..... Eq 4}$$

where P_t is the Rainfall depth in t duration in mm, P_{24} is the rainfall depth in 24-hour duration in mm and t = time duration in hours. Then rainfall in different time intervals for an 8-year return period was utilized for design purposes.

3.2 Preparation of Land Use Land Cover Map

The Land Use Land Cover (LULC) map provides valuable information about the distribution and types of land uses in the region. This map is crucial for assessing the infiltration and runoff attributes of the area, which are particularly relevant for understanding the landscape's hydrological characteristics and potential implications, such as flood risk assessment, urban development planning, and conservation efforts.

The LULC map of the study area for 2022 A.D. was generated using Sentinel imagery in the Google Earth Engine (GEE) platform. The image was selected considering minimum cloud cover and then processed for atmospheric correction. Training samples for the classification were created by visualizing the imagery. Based on the spectral signature of these training points on the image, it was classified into different LULC classes using the supervised classification method called maximum likelihood classification [16].

3.3 Runoff Computation

Traditional theoretical approaches like the Rational Method and NRCS (Natural Resources Conservation Service) curve number method are also in use for stormwater runoff analysis. These methods are more straightforward, making them suitable for quick assessments and smaller-scale projects. The NRCS curve number method, on the other hand, estimates runoff volume by assigning curve numbers to different land use types and soil conditions within a catchment. It is widely used in rural and agricultural. The Rational Method estimates peak runoff rates based on factors such as the intensity and duration of rainfall, catchment area, and runoff coefficient. It is commonly used for small drainage areas and simple calculations. The runoff(Q) from the subcatchment was computed manually using Equation 5 and compared with the outcomes from the model.

$$Q = \frac{\mathrm{C\,I\,A}}{3.6} \qquad \text{…….. Eq 5}$$

Where C is the average runoff coefficient, it is computed using Equation 6, 'I' is the intensity of rainfall in mm/hour and A is the sub-basin area.

$$Cavg = \frac{\mathrm{C1 \times A1 + \ \cdots \ + \ Ci \times Ai}}{\mathrm{A1 + .. + Ai}} \qquad \text{…….. Eq 6}$$

Where C_i is the runoff coefficient for various types of land surfaces and Ai is the area of various types of land surfaces The runoff coefficient was assigned as per NBC 208:2003.

3.4 Modelling and Simulating in SWMM

The modeling of drainage utilizes the open-source software EPA SWMM 5.2. The process begins by importing and geo-referencing the study area image from Google Earth Pro into the software. Subsequently, elements like sub-catchments, nodes, conduits, outfalls, and rain gauges were provided for each sub-catchment. Essential input parameters such as area, slope, width, land use characteristics, and surface roughness were then allocated to these subcatchments to facilitate a complete analysis.

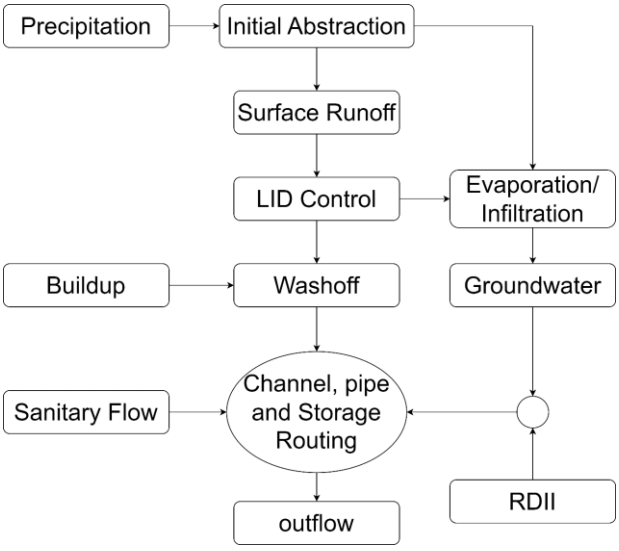

Figure 4:SWMM modelling

Moreover, the modeling process involved specifying critical input parameters, characterizing nodes by invert elevation and maximum depth, and detailing conduits with information like length, cross-sectional dimensions, and surface roughness. Each subcatchment was linked to its predefined node and rain gauge for accurate representation. To accommodate temporal variations, time series rainfall data at one-hour intervals was served into the selected rain gauge. Following this setup, an exhaustive simulation was conducted, evaluating the model's performance based on metrics like maximum flow, capacity, and peak runoff for individual sub-catchments. Within the SWMM framework, adjustments are made to address inadequate capacity through iterative trial processes. The design of conduit sizes and cross-sections throughout the network was carefully considered, with conduits featuring drainage structures and outfalls strategically positioned to optimize cross-sections [17].

Low-impact development (LID) practices were designed to capture surface runoff and provide some combination of detention, infiltration, and evapotranspiration. They were considered as properties of a given sub-catchment. SWMM can explicitly model the following generic types of LID controls: Bio-retention cells, Rain Garden, Green Roofs, Infiltration

Trenches, Continuous Permeable Pavement, Rain Barrel, Rooftop Disconnection and Vegetative Swales [17].

4. Results and Discussions

4.1 Sub-Catchment Delineation of Study Area

The study area was demarcated in Google Earth Pro. The entire catchment was divided into 13 sub-catchments based on the slope, elevation, drainage pattern, roadways, and collective flow path of the runoff generated from the sub-catchments. The different catchment areas are shown in Figure 5.

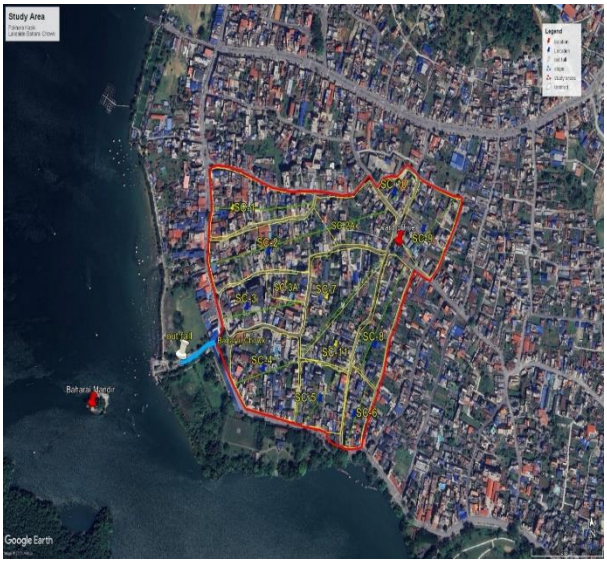

Figure 5: Sub-catchment division of the study area

The details of the different sub-catchments along with various parameters of the study area is given in Table 1.

Table 1: Geometric properties of the sub-catchments

S.N	Sub-Catchments	Area (ha)	Width (m)	Slope %
1	SC-1	2.58	110	4.7
2	SC-2	3.5	113	6.1
3	SC-2A	1.6	106	4.9
4	SC-3	1.56	133	4.4
5	SC-3A	0.61	109	4.5
6	SC-4	3.1	181	4.5
7	SC-5	1.74	125	6.2
8	SC-6	0.97	67	4.4
9	SC-7	2.6	166	4.7
10	SC-8	1.91	80	4.9
11	SC-9	2.13	127	5.2
12	SC-10	0.6	81.8	4.3
13	SC-11	2.5	102	4.5

Among the 13 sub-catchments of the study area, the maximum and minimum slopes were 6.2% and 4.3%, respectively. The maximum area of a sub-catchment was 3.5 hectares for SC-2, and the minimum area was 0.6 hectares for SC-10.

4.2 Precipitation Data Analysis

The daily rainfall data of the meteorological station at Pokhara airport (station number 804) from 2000-2022 A.D. obtained from the DHM was analyzed to compute design rainfall for the drainage structures.

Table 2: Comparison of Cross-section of Existing and Modified of Drain

Year	Maximum 24-hour Rainfall depth in mm	Year	Maximum 24-hour Rainfall depth in mm
2000	217.2	2011	168.2
2001	357	2012	173.5
2002	211.5	2013	223.5
2003	177.2	2014	218.3
2004	171.3	2015	223.7
2005	166	2016	274.2
2006	109.2	2017	191.4
2007	227.2	2018	207
2008	151.7	2019	107.5
2009	247.7	2020	250.9
2010	262.1	2021	280
		2022	177.2

In Table 2 above, the year 2001 A.D. was identified as having the maximum twenty-four-hour rainfall, with a rainfall depth of 357 mm, while the minimum twenty-four-hour rainfall, with a depth of 107.9 mm was found in the year 2019 A.D., over the last two decades.

The maximum twenty-four-hour duration rainfall of each year was disaggregated into small time intervals (5 minutes, 10 minutes, 15 minutes, 2 hours, etc.). Then, using Gumbel's Extreme Value Distribution, eight-year return period rainfall data for different time intervals were computed, which were used as rainfall for modeling in drainage. Figure 6 below shows the computed intensity-duration curve for the study area.

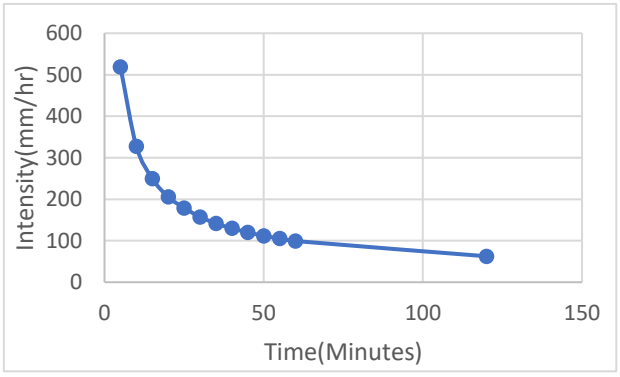

Figure 6: Intensity Duration Curve for the Study Area

4.3 Land Use Land Cover Map

A land use and land cover map were prepared using Sentinel imagery from the year 2022 via Google Earth Engine (GEE) with supervised classification. Ground truth data representing various land cover classes were gathered to effectively train the supervised classification algorithm. Maximum likelihood classification algorithms
were applied to utilize the spectral information from the Sentinel imagery and the ground truth data to categorize pixels into specific land use and land cover classes.

The completed land use and land cover map provides comprehensive coverage of the study area, accurately categorizing various land cover classes based on the Sentinel imagery and ground truth data. The accuracy assessment confirmed the reliability of the classification results, demonstrating the effectiveness of the supervised classification approach.

A comprehensive Land Use Land Cover map for the study area, along with its sub-catchments and corresponding land use percentages, is visually depicted in Figure 7. Additionally, the percentage of each class of land use and land cover in each sub-basin is presented in Table 3.

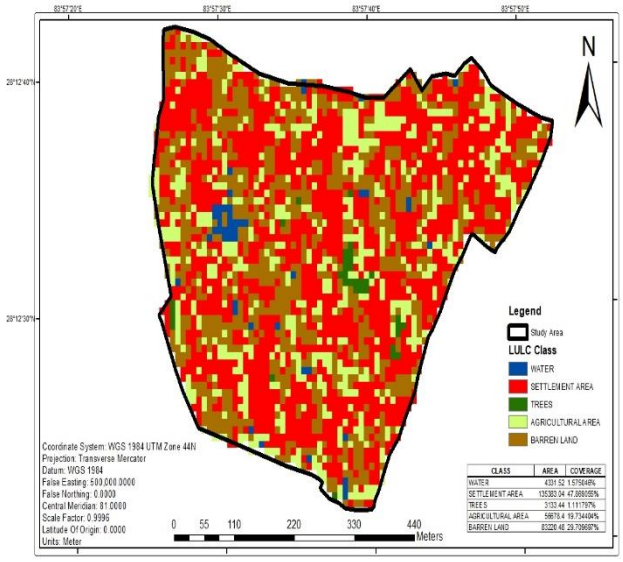

Figure 8: LULC map of study area obtained from GEE.

Table 3: LULC according to sub-catchment

Descriptions	Settlement	Tree	Agriculture	Barren Land	Water
Total Area	**47.86%**	**1.11%**	**19.73%**	**29.71%**	**1.51%**
CS-1	42.7%	0%	13.16%	43.77%	0.35%
CS-2	48.91%	0.27%	17.93%	31.79%	1.06%
CS-2A	51.86%	0%	26.97%	20.74%	0.41%
CS-3	34.59%	0%	21.32%	36.96%	7.1%
CS-3A	52.17%	1.45%	13.04%	31.86%	1.44%
CS-4	48.03%	0.3%	18.73%	31.17%	1.61%
CS-5	55.08%	0%	20.32%	22.45%	2.13%
CS-6	47.16%	0%	20.75%	30.18%	1.88%
CS-7	48.36%	4.36%	20%	25.82%	1.45%
CS-8	51.21%	3.38%	22.22%	22.70%	0.48%
CS-9	57.26%	0%	23.78%	18.94%	0%
CS-10	62.12%	0%	9.09%	27.27%	1.51%
CS-11	49.12%	3.29%	20.87%	26.37%	0%

4.4 SWMM Simulation

For the analysis, EPA SWMM 5.2 software was adopted. First, the different components of the drainage networks were defined, including sub-catchments, rainfall data, conduits, nodes, junctions, and outfalls. The area, slope, impervious percentage, and rainfall intensity were assigned to the respective elements of the model.

The simulation for the existing network showed that all of the drainage systems are overloaded for the design rainfall events. Their capacity has been utilized 100%. Therefore, drainage networks are not capable of carrying runoff volume properly. The outcomes of the simulation are illustrated in Figure 8. The

analysis indicates that the existing drainage networks can't accommodate runoff from the catchment. Either there is a need to increase the drainage size or implement methods suitable for reducing runoff from the surrounding area.

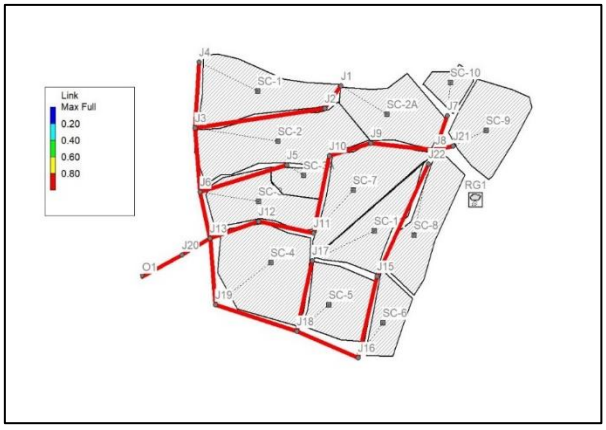

Figure 7: Status of existing drainage network during maximum rainfall

The entire cross-sections of the drainage were increased to fully accommodate and discharge the runoff without overflow. The existing drain and increased SWMM design cross-sections are shown in Table 4, and the outcomes of the simulation for modified drainage are represented in Figure 9. After the modification of the drainage, they were able to accommodate runoff; however, their cross-sections are too large to implement in the study area due to existing infrastructures. This resulted in the requirement of an alternative solution to reduce peak runoff discharge so that the existing drainage could handle the situation with ease.

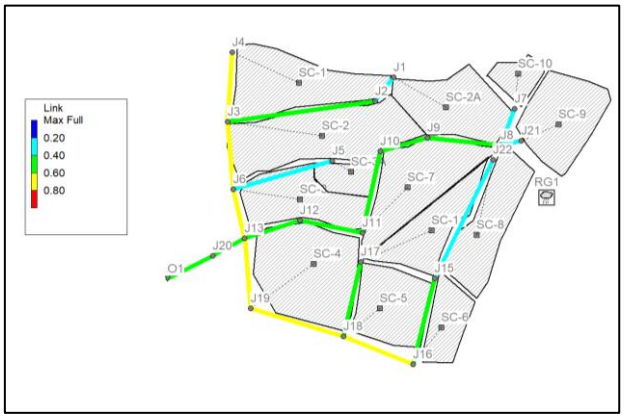

Figure 8: Status of drainage network during maximum rainfall after modification

Table 4: Comparison of Cross-section of Existing and Modified of Drain

S. N.	Channel	Cross Sections in meters (width X depth)		Side Alignment to Roadway
		Existing (Tick Drain)	SWMM Design (Closed Rectangular)	
1	CH-1	0.1×0.2	0.3×0.5	Both sides
2	CH-2	0.1×0.2	0.3×0.5	Both sides
3	CH-3	0.1×0.2	0.5×0.8	Both sides
4	CH-4	0.1×0.2	0.5×0.95	Both sides
5	CH-5	0.1×0.2	0.5×1	Both sides
6	CH-6	0.1×0.2	0.5×1	Both sides
7	CH-7	0.1×0.2	0.5×1	Both sides
8	CH-8	0.1×0.2	0.5×1	Both sides
9	CH-9	0.1×0.2	0.5×1	Both sides
10	CH-10	0.1×0.2	0.5×1	Both sides
11	CH-11	0.1×0.2	0.5×1	Both sides
12	CH-12	0.1×0.2	0.5×0.8	Both sides
13	CH-13	0.1×0.2	0.5×0.8	Both sides
14	CH-14	0.1×0.25	0.5×0.8	Both sides
15	CH-15	0.1×0.25	0.7×1.5	Both sides
16	CH-16	0.1×0.25	1×2	Both sides
17	CH-17	0.1×0.25	1×2	Both sides
18	CH-18	0.1×0.25	1×2.2	Both sides
19	CH-19	0.1×0.25	1×2.5	Both sides
20	CH-20	0.1×0.25	1×2.5	Both sides
21	CH-21	0.1×0.25	1×2.5	Both sides

4.5 Validation of the Model

The hydraulic models are difficult to validate, especially roadside flood modeling, due to the lack of runoff depth or discharge measurements, unlike the river network, which has gauge stations for measurement. Therefore, in this study, the outcomes of SWMM were compared with manual computations of drainage size using Manning's equation. Both the manual computation and SWMM model resulted in similar dimensions of drainage. The cross-section from SWMM was 0.5m × 1.1m. That is similar to the cross-section of 0.5m x 0.94m computed using Manning's equation for rational peak runoff.

4.6 Rain Garden Modelling and Simulation

Rain gardens of varying dimensions, including 6m x 2m, 6m x 2.5m, and 4m x 3m, were strategically assigned within each sub-catchment of the study area, considering factors such as area size and flow patterns. Approximately 3% of the impervious surface area within each sub-catchment was transformed into these rain gardens. These rain gardens were strategically located in public open concrete spaces,

residential and commercial open areas, as well as alongside road rights-of-way. For the rain garden design, soil with an initial infiltration rate of 30 mm/hr, a minimum depth of 300 mm, and a berm height of 300 mm were considered. Simulations using SWMM with the inclusion of rain gardens greatly reduced runoff volume and peak runoff. Detailed results are available in Table 5. These rain gardens could play a crucial role in mitigating stormwater runoff and enhancing the overall environmental sustainability of the study area.

Table 5: Model Outcomes for Rain Garden Simulation

SN	Sub Catchment	Total Runoff 10^6 lit	Peak Runoff CMS	Total Runoff 10^6 lit	Peak Runoff CMS	Difference in Total runoff %	Difference in Peak runoff %
		Without Rain Garden		With Rain Garden			
1	SC-1	4.74	2.66	4.46	2.16	5.91 %	18.80 %
2	SC-2	6.74	4.01	6.28	3.21	6.82 %	19.95 %
3	SC-2A	3.07	1.98	2.86	1.55	6.84 %	21.72 %
4	SC-3	2.99	1.96	2.79	1.52	6.69 %	22.45 %
5	SC-3A	1.63	1.09	1.52	0.84	6.75 %	22.94 %
6	SC-4	5.96	3.78	5.56	2.98	6.71 %	21.16 %
7	SC-5	3.34	2.19	3.11	1.7	6.89 %	22.37 %
8	SC-6	1.86	1.2	1.74	0.94	6.45 %	21.67 %
9	SC-7	4.99	3.21	4.66	2.51	6.61 %	21.81 %
10	SC-8	3.67	2.34	3.43	1.84	6.54 %	21.37 %
11	SC-9	4.09	2.64	3.81	2.06	6.85 %	21.97 %
12	SC-10	1.15	0.77	1.07	0.59	6.96 %	23.38 %
13	SC-11	4.82	2.91	4.49	2.331	6.85 %	19.90 %

The conversion of about 3% of impervious areas of each sub-catchment into a Rain Garden showed an average reduction of 21.50% of peak runoff and 6.68% of total runoff from sub-catchments in SWMM simulation. This showed the effectiveness of the Rain Garden in the peak runoff thus, reduction of hydraulic loading of urban drainage during the short duration of high intense rainfall.

4.7 Permeable Pavement Modelling and Simulation

Similarly, the model was simulated by assigning permeable pavement based on the impervious area. The road footpaths along both sides of the road were studied for their suitability and applicability to permeable pavement, which we had allocated for both purposes: footpath and permeable pavement. The total area, thickness, and soil properties were the major parameters assigned for the design of permeable pavement. This study utilized 5% of impervious area transformed into permeable pavement for the modeling. After incorporating all these parameters into SWMM, simulation and analysis were performed. The outcomes of the simulation using permeable concrete are shown in Table 6.

Table 5: Model Outcomes for Permeable Pavement

SN	Sub Catchment	Total Runoff 10^6 lit	Peak Runoff CMS	Total Runoff 10^6 lit	Peak Runoff CMS	Difference in Total runoff %	Difference in Peak runoff %
		Without Permeable Pavement		With Permeable Pavement			
1	SC-1	4.74	2.66	4.35	2.07	8.23 %	22.18 %
2	SC-2	6.74	4.01	6.08	3.11	9.79 %	22.44 %
3	SC-2A	3.07	1.98	2.8	1.48	8.79 %	25.25 %
4	SC-3	2.99	1.96	2.69	1.48	10.03 %	24.49 %
5	SC-3A	1.63	1.09	1.49	0.82	8.59 %	24.77 %
6	SC-4	5.96	3.78	5.49	2.88	7.89 %	23.81 %
7	SC-5	3.34	2.19	3.05	1.64	8.68 %	25.11%
8	SC-6	1.86	1.2	1.69	0.9	9.14 %	25.00 %
9	SC-7	4.99	3.21	4.52	2.41	9.42 %	24.92 %
10	SC-8	3.67	2.34	3.31	1.75	9.81 %	25.21 %
11	SC-9	4.09	2.64	3.72	1.97	9.05 %	25.38 %
12	SC-10	1.15	0.77	1.03	0.58	10.43 %	24.68 %
13	SC-11	4.82	2.91	4.35	2.21	9.75 %	24.05 %

The conversion of approximately 5% of impervious areas in each sub-catchment into Permeable Pavement resulted in an average reduction of 24.41% in peak runoff and 9.2% in total runoff from the sub-catchment area in the SWMM simulation. This demonstrates the effectiveness of Permeable Pavement in reducing peak runoff during short-duration, high-intensity rainfall events. The hydraulic loading in the conduit was significantly reduced during peak flow by implementing permeable concrete in urban areas.

4. Conclusion

The study focuses on analyzing urban road flooding in Pokhara Metropolitan City, particularly the Bharai Chowk Road section, using SWMM modeling for mitigation purposes. SWMM analysis revealed that the existing drainage network cannot handle the generated peak runoff during intense rainfall. The drainage canals, mostly tick drains, are undersized, and existing conduits are almost full, indicating the need for redesigning and resizing drainage structures. Introducing rain gardens and permeable pavement in each sub-catchment significantly reduces peak and total runoff. Rain gardens alone reduce peak runoff

by 16-20% and total runoff by 5-7% when implemented on 3% of the impervious area. The study identifies high rainfall intensity, impervious areas, and inadequate drainage systems as the main causes of urban road flooding. Implementing low-impact development (LID) controls such as rain gardens and permeable pavement, along with resizing existing drainage, can mitigate urban road flooding. Policymakers, practitioners, and stakeholders need to actively address these issues to mitigate urban road flooding and promote sustainable urbanization.

Acknowledgment

The authors acknowledge Dr. Binaya Mishra of Pokhara University for their valuable comments and suggestions to improve this manuscript. Also, we want to appreciate the dedication of the anonymous reviewer, whose effort helped to organize and streamline the manuscript.

References

[1] Karki, R., Talchabhadel, R., Aalto, J., and Baidya, S. K. New climatic classification of Nepal. Theor. Appl. Climatol., 125(3) (2016) 799–808. doi: 10.1007/s00704-015-1549-0.

[2] Posthumus, H., Hewett, C.J.M., Morris, J., Quinn, P.F. Agricultural land use and flood risk manage-ment: Engaging with stakeholders in North York-shire. Agric. Water Manag. 95(2008) 787–798. https://doi.org/10.1016/j.agwat.2008.02.001

[3] Muzzini, E., Aparicio, G. Urban growth and spatial transition: an initial assessment. World Bank, Washington, D.C (2013)

[4] Shuster, W.D., Bonta, J., Thurston, H., Warnemuende, E., Smith, D.R., 2005. Impacts of impervious surface on watershed hydrology: A review. Urban Water 2(4) (2005) 263–275. https://doi.org/10.1080/15730620500386529

[5] Skougaard Kaspersen, P., Høegh Ravn, N., Arnbjerg-Nielsen, K., Madsen, H., Drews, M. Influence of urban land cover changes and climate change for the exposure of European cities to flood-ing during high-intensity precipitation. Proc. Int. Assoc. Hydrol. Sci., 370 (2015) 21–27, https://doi.org/10.5194/piahs-370-21-2015

[6] Luo, P., Luo, M., Li, F., Qi, X., Huo, A., Wang, Z., He, B., Takara, K., Nover, D., Wang, Y., Urban flood numerical simulation: Research, methods and future perspectives. Environ. Model. Softw. 156 (2022), https://doi.org/10.1016/j.envsoft.2022.105478

[7] Pour, S.H., Wahab, A.K.A., Shahid, S., Asaduzzaman, M., Dewan, A. Low impact development techniques to mitigate the impacts of climate-change-induced urban floods: Current trends, issues and challenges. Sustain. Cities Soc., 62 (2020) 102373. https://doi.org/10.1016/j.scs.2020.102373

[8] Singh, A., Sarma, A.K., Hack, J. Cost-Effective Optimization of Nature-Based Solutions for Reduc-ing Urban Floods Considering Limited Space Avail-ability. Environ. Process, 7 (2020) 297–319, https://doi.org/10.1007/s40710-019-00420-8

[9] Tsihrintzis, V.A., Hamid, R. Runoff quality predic-tion from small urban catchments using SWMM. Hydrol. Process, 12 (1998) 311–329. https://doi.org/10.1002/(SICI)1099-1085(199802)12:2<311::AID-HYP579>3.0.CO;2-R

[10] Boonya-aroonnet, S., Weesakul, S., Mark, O. Modeling of Urban Flooding in Bangkok, in: Global Solutions for Urban Drainage. Presented at the Ninth International Conference on Urban Drainage (9ICUD), American Society of Civil Engineers, Lloyd Center Doubletree Hotel, Portland, Oregon, United States 9 (2002) 1–14. https://doi.org/10.1061/40644(2002)274

[11] Rangari, V.A., Umamahesh, N.V., Bhatt, C.M. Assessment of inundation risk in urban floods us-ing HEC RAS 2D. Model. Earth Syst. Environ 5 (2019) 1839–1851. https://doi.org/10.1007/s40808-019-00641-8

[12] Khadka, S., Basnet, K. Storm Water Management of Barahi Chowk Area, Lakeside, Pokhara, Nepal using SWMM. KEC Conf. Proc. 2 (2019).

[13] Paudel, S., Dawadi, N.P. Stormwater Analysis and Drainage Management in Pokhara Metropolitan City, Nepal. IOE Graduate Conference. 12 (2022).

[14] Chattamvelli, R., Shanmugam, R. Gumbel Distri-bution, in: Continuous Distributions in Engineer-ing and the Applied Sciences – Part II, Synthesis Lectures on Mathematics & Statistics. Springer International Publishing, Cham, (2021) 263–271, https://doi.org/10.1007/978-3-031-02435-1_11

[15] Mahdi, E.S., Mohamedmeki, M.Z. Analysis of rain-fall intensity-duration-frequency (IDF) curves of Baghdad city. IOP Conf. Ser. Mater. Sci. Eng., 888 (2020) 012066. https://doi.org/10.1088/1757-899X/888/1/012066

[16] Nasiri, V., Deljouei, A., Moradi, F., Sadeghi, S.M.M., Borz, S.A., 2022. Land Use and Land Cover Map-ping Using Sentinel-2, Landsat-8 Satellite Images, and Google Earth Engine: A Comparison of Two Composition Methods. Remote Sens., 14 (2008) 1977. https://doi.org/10.3390/rs14091977

[17] Rossman, L.A., 2016. Storm Water Management Model Reference Manual Volume I – Hydrology (Revised), (2016).